JOC The Journal of Organic Chemistry
Article
pubs.acs.org/joc

The "Case of Two Compounds with Similar Configuration but Nearly Mirror Image CD Spectra" Refuted. Reassignment of the Absolute Configuration of *N*-Formyl-3′,4′-dihydrospiro[indan-1,2′(1′*H*)-pyridine]

Daniele Padula,[‡,†] Lorenzo Di Bari,[‡] and Gennaro Pescitelli*[,‡]

[‡]Dipartimento di Chimica e Chimica Industriale, Università di Pisa, via Moruzzi 13, 56124 Pisa, Italy

[†]Department of Chemistry, University of Warwick, Gibbet Hill Road, CV4 7AL Coventry, U.K.

Supporting Information

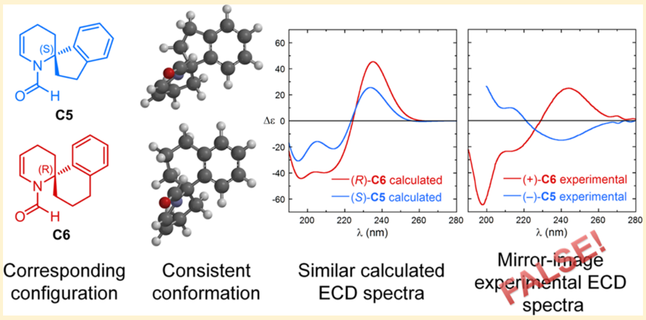

ABSTRACT: In 1997, Sandström and co-workers reported the case of two chiral spiro compounds with very similar skeletons but showing almost mirror-image electronic circular dichroism (ECD) spectra for the corresponding absolute configuration. The paper has been often cited as a proof and good educational example of the pronounced sensitivity of ECD toward molecular conformation, and a clear warning against the use of ECD spectral correlations to assign absolute configurations. Although both concepts remain valid, they are not exemplified by the quoted paper. We demonstrate that the original configurational assignment of one compound was wrong and revise it by using TDDFT calculations. The main reason for the observed failure is the use of the matrix method, a popular approach to predict ECD spectra of compounds which can be treated with an independent system approximation (ISA), including proteins. Using a modern version of the matrix method, we demonstrate that the ISA is not valid for the title compound. Even in the absence of apparent conjugation between the component chromophores, the validity of the ISA should never be taken for granted and the effective extent of orbital overlap should always be verified.

■ INTRODUCTION

Chiroptical spectra such as electronic and vibrational circular dichroism (ECD and VCD, respectively) are observed upon the interaction of chiral nonracemic substances with circularly polarized radiation.[1] A widely accepted notion in the context of chiroptical spectra is their enhanced dependence and sensitivity on the molecular conformation, especially in comparison with their achiral counterparts such as UV−vis absorption and IR. This is because the fundamental quantity responsible for ECD and VCD signals, that is the rotational strength, depends on the scalar product between electric and magnetic transition dipoles.[1] Therefore, the intensity and the sign of each ECD or VCD band intrinsically contain geometrical information: namely, the angle between the two transition dipoles. This is in contrast with UV−vis and IR spectra, which depend on the square of the electric transition dipole only and for this reason are rather insensitive to stereochemical issues. More often than one would expect, the electric and magnetic transition dipoles happen to be almost perpendicular to each other; therefore, any small variation in the molecular geometry or in the dipole direction may affect not only the intensity but even the sign of a CD band, while leaving the absorption spectrum unaffected.

This enhanced sensitivity of ECD, VCD, and other chiroptical properties toward conformation is especially evident in biochemistry and biophysics, where these techniques are mostly employed to study the secondary structure of biopolymers such as proteins, peptides, and nucleic acids.[2] In addition in the context of small molecules, chiroptical spectra may lend themselves as tools to study the molecular conformation.[3,4] Conversely, when these techniques are employed to assign absolute configurations, an accurate knowledge of the conformational situation must be obtained as a necessary prerequisite. Several examples are available of the influence of conformation on experimental and calculated ECD or VCD spectra.[5−11] A spectacular example was reported in 1997 by Sandström and co-workers concerning the two spiro compounds **C5** and **C6** (Chart 1, denoted **3** and **2** in the original paper).[12] They differ only in the length of the CH_2 bridge and therefore in the size of the saturated ring (five- vs six-membered). Otherwise, the remaining molecular portions are the same: in particular, the two chromophoric moieties are identical (1,2-disubstituted benzene ring and *N*-formylvinylamine). It was therefore expected that the two compounds (*S*)-**C5** and (*R*)-**C6**, with the same configuration at the spiro center, would show very similar ECD spectra (note in Chart 1 the

Received: June 13, 2016
Published: July 27, 2016

DOI: 10.1021/acs.joc.6b01416
J. Org. Chem. 2016, 81, 7725−7732

Chart 1. Compounds C5 (Denoted 3 in the Original Paper) and C6 (2)

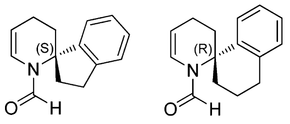

C5 **C6**

formal inversion of chirality according to the Cahn−Ingold−Prelog sequence rule). In contrast, (*S*)-**C5** and (*R*)-**C6** were associated with almost mirror-image ECD spectra.[12,13] This very surprising result was achieved by means of ECD calculations run with the so-called Schellman matrix method,[14,15] a popular calculation approach at that time, based on the independent system approximation (ISA).[16] In the ISA framework, a multichromophoric molecule is partitioned in "independent systems": that is, chromophoric moieties with negligible orbital overlap. The diverse electronic excitations of the various chromophores are considered to couple through space: i.e., through the Coulombic interaction between their transition densities. All possible interactions can be considered simultaneously and to all-order by means of a matrix method such as that of Schellman[14−16] (details can be found in the Results and Discussion).

Sandström and co-workers employed the matrix method to calculate ECD spectra and assign the absolute configurations of the two spiro compounds **C5** and **C6**.[12,13] These latter compounds had been synthesized as racemate mixtures and separated by enantioselective GLC;[12] therefore, the only proof of the absolute configuration came from the comparison of experimental ECD spectra with those obtained with the aforementioned matrix method. As noted above, the calculated ECD spectra turned out to be nearly mirror images for (*S*)-**C5** and (*R*)-**C6**, with the same configuration at the spiro center. The most important conclusion from the paper was that "the result is a caveat against deducing identity in absolute stereochemistry from strong similarity between CD spectra":[12] i.e., against the use of the so-called ECD spectral correlations. In fact, the paper has been frequently quoted in the following years as an example of a clear warning against the use of ECD spectral correlations.[17−24] The authors attributed the different ECD spectra of **C5** and **C6** to a slightly different conformation adopted by the two compounds (see discussion below for more details). Thus, the paper also offered a strong proof of the pronounced sensitivity of ECD toward the molecular conformation[13,23,25] and lent itself as a good example for educational purposes.[26] The very instructive lesson from the paper was that ECD spectra reflect the overall absolute stereochemistry, not only the absolute configuration as often believed.

During the preparation of the teaching material for a graduate course in Stereochemistry at the University of Pisa, we again came across the two spiro compounds as a good educational example of the relation between conformation, configuration, and ECD spectra. With the aim of showing optimized geometries during the lectures, we ran a standard conformational analysis procedure with molecular mechanics (MM) and density functional theory (DFT). The structures we obtained were similar to those reported in the original paper (see discussion below); however, they also looked much more consistent between the two compounds than we expected. This prompted us to run ECD calculations with modern means: that is, time-dependent DFT (TDDFT).[27] To our surprise, the TDDFT calculated ECD spectrum for (*S*)-**C5** was very different from that calculated with the Schellman method reported in the original paper and actually looked as its mirror image.[12] As a consequence, the absolute configuration originally assigned to *N*-formyl-3′,4′-dihydrospiro[indan-1,2′(1′*H*)-pyridine] (**C5**) was wrong and needed to be revised. More importantly, the textbook example of "a case of two compounds with similar configuration but nearly mirror image CD spectra"[12] was refuted. Our analysis demonstrates that the main source of the error in the original investigation lies in the fact that the aromatic and *N*-formyl enamine chromophores are not independent in the sense implied by the ISA; therefore, the ECD spectra of both compounds **C5** and **C6** cannot be correctly treated by the matrix method approach.

■ RESULTS AND DISCUSSION

Conformational Searches and Geometry Optimizations. Our consolidated conformational analysis/geometry optimization procedure consists of two steps:[27] (a) a thorough conformational search run with the Monte Carlo algorithm and the molecular Merck force field (MMFF) and (b) reoptimization of all energy minima found in step (a) by DFT. In the current case, DFT geometry optimizations were run at the ωB97X-D/6-311+G(d,p) level. The results are summarized in Figure 1. Only two conformers were found for both compounds (*S*)-**C5** and (*R*)-**C6** with significant population at 300 K (>5%), while two other energy minima were obtained in both cases with populations between 1% and 2.5%. The two most stable conformers (labeled conf#1 and conf#2) differ from each other in the conformation assumed by the five- or the six-membered ring. DFT minima and relative energies are compared in Figure 1 with the minima and energies shown in the original paper (labeled **2a**,**b** and **3a**), which were calculated with the MM2(91) force field.[12] We noticed that for compound **C6** the first two DFT geometries (**C6** conf#1 and conf#2) correspond to the MM2 minima (**2b** and **2a**), although with reversed relative stability. For compound **C5**, the DFT absolute

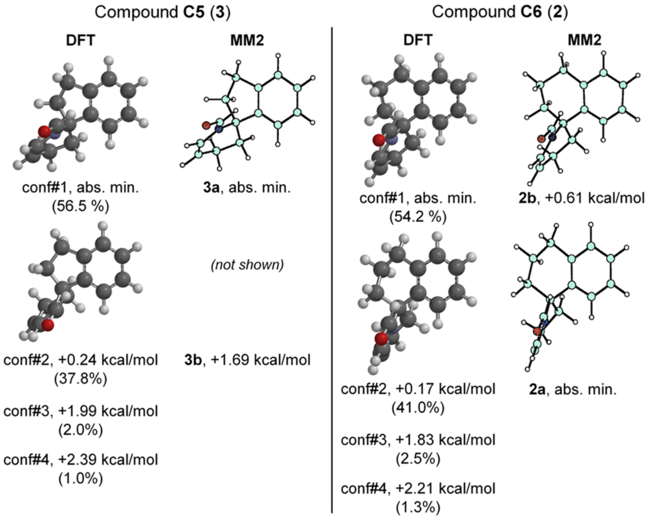

Figure 1. Structure, relative energies, and Boltzmann population at 300 K calculated for the most stable conformers of compounds (*S*)-**C5** and (*R*)-**C6** with DFT (ωB97X-D/6-311+G(d,p), present work) and MM2 (adapted with permission from ref 12, copyright 1997 American Chemical Society). MM2 minima are labeled as in the original work.

minimum (**C5** conf#1) corresponds to the MM2 minimum (**3a**), apart from a less pronounced puckering of the five-membered ring which is overestimated by MM2.

In contrast, the second DFT minimum (**C5** conf#2) was not found by MM2, or at least it was not associated with the high population found by DFT (the structure for the second most stable conformer labeled **3b** is not reported in the paper and this conformer was neglected in ECD calculations due to its small population).[12] It is also apparent from our DFT structures that the geometries of the most stable conformers (**C5** conf#1 and **C6** conf#1) are consistent with each other for what concerns the reciprocal arrangement of the aromatic and *N*-formyl enamine chromophores. The same is true for the second most stable conformers (**C5** conf#2 and **C6** conf#2). In the original paper, the authors stressed the structural difference between the most stable conformers for the two compounds: namely, **2a** and **3a** in their case (Figure 1).[12] In our structures, such a difference is not so evident, especially taking into account the presence of a second minimum for **C5** and the calculated energy order for the two conformers of each compound. In conclusion, the conformational situation emerging from DFT geometry optimizations is much more homogeneous than that emerging from MM2 calculations in the original paper.[12] For this reason we did not expect any strong difference between the ECD spectra calculated for the two compounds.

ECD Calculations with TDDFT. TDDFT calculations were run on all DFT energy minima with population >1% at 300 K: i.e., four conformers for each compound. TDDFT calculations were run with different functionals (B3LYP, CAM-B3LYP, M06-2X) and the def2-TZVP basis set. The calculation results obtained with various functionals were all consistent with each other; CAM-B3LYP results are discussed in the following. The ECD spectra calculated for (*S*)-**C5** and (*R*)-**C6** after Boltzmann averaging at 300 K are shown in Figure 2 and compared with the experimental spectra measured on (−)-**C5** and (+)-**C6** in ethanol, reported in ref 12. The results of calculations with other functionals (B3LYP and M06-2X), as well as of calculations run at CAM-B3LYP/def2-TZVP using the polarizable continuum model (PCM) for ethanol,[28,29] are shown in Figures S1 and S2 in the Supporting Information.

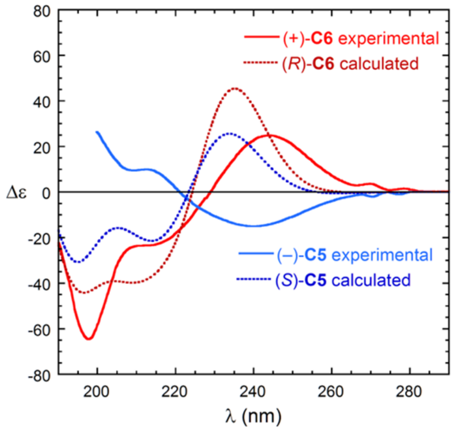

Figure 2. Solid traces giving experimental ECD spectra of compounds (−)-**C5** and (+)-**C6** in ethanol (adapted with permission from ref 12, copyright 1997 American Chemical Society) and dotted traces giving ECD spectra calculated for compounds (*S*)-**C5** and (*R*)-**C6** at the CAM-B3LYP/def2-TZVP level in vacuo as a Boltzmann average over four conformers optimized at the *ω*B97X-D/6-311+G(d,p) level. Spectra are convoluted as sums of Gaussians with 0.3 eV exponential half-width, shifted to the red by 10 nm.

It appears that the ECD spectra calculated for (*S*)-**C5** and (*R*)-**C6** with the same configuration at the spiro center are very similar to each other, and they are not at all "nearly mirror images" of each other as suggested in the original paper. TDDFT calculations are able to reproduce the experimental ECD spectra of the two spiro compounds satisfactorily. In both cases, the relative sequence of signs, band energies, and intensities is correctly predicted by the calculations. The experimental spectrum of (+)-**C6** is in accord with the calculated spectrum for (*R*)-**C6**; therefore, the configuration of this compound is confirmed as (+)-(*R*)-**C6**. On the other hand, the experimental ECD spectrum of (−)-**C5** is almost the mirror image of the spectrum calculated for (*S*)-**C5**. This means that the absolute configuration assignment of compound **C5** from the original paper, namely (−)-(*S*)-**C5**,[12] must be reversed, and the correct absolute configurations are (−)-(*R*)-**C5** and (+)-(*S*)-**C5**. The assignments were also confirmed by optical rotation calculations run at the CAM-B3LYP/def2-TZVP//*ω*B97X-D/6-311+G(d,p) level including PCM for ethanol. The calculated $[\alpha]_D$ values (Boltzmann averages over four conformers in each case) were +77.0 for (+)-(*R*)-**C6** and +86.2 for (+)-(*S*)-**C5**. These values compare well with experimental ones: namely, +55.2 for (*R*)-**C6** (ethanol, optically pure) and +16.4 for (+)-**C5** (ethanol, 16% ee) or −35.9 for (−)-**C5** (ethanol, 37% ee).[12] It is not infrequent that "old" configuration assignments of organic compounds are reversed in recent times thanks to the modern calculation approaches of ECD, VCD, and optical rotation.[30] Note that since the enriched or pure enantiomers of (*S*)-**C5** and (*R*)-**C6** were obtained by enantioselective GLC, Sandström and coworkers had no independent hint of the correct absolute configuration.[12] Because two different stationary phases were used, moreover, even the questionable proof of the elution orders was not available as a guide to the absolute configuration assignment.

The use of different functionals (B3LYP and M06-2X) led to calculated ECD spectra consistent with those obtained with CAM-B3LYP (see Figure S1 in the Supporting Information). In particular, Boltzmann-averaged ECD spectra calculated at the M06-2X/def2-TZVP level are almost superimposable with CAM-B3LYP/def2-TZVP results and are in very good agreement with experimental spectra. Similarly, the inclusion of a solvent model (PCM for ethanol) in CAM-B3LYP/def2-TZVP calculations had practically no effect on the final outcome, in particular for (*S*)-**C5** (see Figure S2 in the Supporting Information). These results demonstrate that TDDFT ECD calculations with "good" functionals[27] such as CAM-B3LYP and M06-2X are accurate enough to predict the ECD of the spiro compounds **C5** and **C6**. A worse agreement was instead observed by using the B3LYP functional, although the same conclusion about the absolute configuration assignments would be reached. In fact, average spectra calculated at the B3LYP/def2-TZVP level showed a splitting of the first positive ECD band, which is apparent neither in the experimental spectra nor in those calculated with the other functionals (see Figure S1 in the Supporting Information). The less satisfying behavior of B3LYP is associated with the charge-transfer (CT) character of some of the calculated transitions, as is discussed below. It is known that B3LYP and other global hybrids with small HF exchange fraction afford a poor description of CT-like states because of an incorrect asymptotic behavior.[31−34]

ECD Calculations with Matrix Method (EXAT). The matrix method for the calculation of absorption and ECD spectra of multichromophoric systems is based on the expression of the excited states of the system as a linear combination of local excitations: i.e., excitations localized on the component chromophores.[14−16] In the matrix formulation, this is achieved by resolving an eigenvalue problem: that is, by expressing the Hamiltonian of the system as a square matrix in which the diagonal elements are the excitation energies of the local excitations and the off-diagonal elements represent the Coulombic interactions between all possible pairs of transitions on the various chromophores. The properties of the multichromophoric system are retrieved by combining the properties of the single chromophores through the eigenvector matrix.[14−16] The local excitation energies used as diagonal elements can be extracted from experimental data or from calculations on chromophoric models. The first option was employed by Sandström and co-workers in the original paper, while we employed TDDFT calculations (see below). Off-diagonal elements are normally not accessible experimentally and must be estimated computationally. In the traditional approach, transition densities are either approximated as point dipoles or expressed in terms of point transition charges (charge monopoles) localized on atoms.[16,35] This latter approach was used by Sandström and co-workers,[12] who estimated atom-centered charge monopoles with the semiempirical AM1 method. The point charge approximation is known to perform relatively well for large molecules with extended chromophores, for which the number of points used to evaluate the transition density is high.[36] In the current case, however, the small molecular size and nature of chromophores suggested the use of a more refined approach based on full transition densities to avoid the errors associated with their discretization over a small number of points.[37]

In their matrix-method calculations on compounds **C5** and **C6**,[12] Sandström and co-workers included the main transitions for the 1,2-disubstituted benzene and *N*-formylvinylamine chromophores: that is, four $\pi \rightarrow \pi^*$ transitions of the 1,2-disubstituted benzene (^1L_b, ^1L_a, ^1B_b, and ^1B_a) and the $n \rightarrow \pi^*$ and $\pi \rightarrow \pi^*$ transitions of *N*-formylvinylamine. The set of transition point charges was extracted from AM1 calculations on 1,2-dimethylbenzene and *N*-formylvinylamine as model chromophores. The full set of data are given in Table 1 of ref 12 and they are replicated in Table S1 in the Supporting Information. We wish to comment that despite the approximated method of calculation (semiempirical AM1 level of theory), the set of data looks very reasonable in comparison with our TDDFT calculations. Using the same model chromophores, we ran TDDFT calculations at the CAM-B3LYP/def2-TZVP level of theory and obtained a set of transition point charges by fitting the electrostatic potential generated by the TDDFT transition density, according to the Merz−Kollman scheme.[38,39] The main discrepancy between AM1 and TDDFT-based transition point charges is the zero transition charge found by AM1 for both N and C(=O) atoms for the $\pi \rightarrow \pi^*$ transition of the *N*-formylvinylamine chromophore,[12] which is contradicted by our results (see Figure S3 in the Supporting Information).

In the original paper,[12] matrix-method calculations were run on a single conformer for compound **C5** (labeled **3a**) and two conformers for **C6** (labeled **2a**,**b**). The comparison with experimental spectra (Figure 3 of ref 12, replicated in the present Figure S4 in the Supporting Information) led to the following configurational assignments: (+)-(*R*)-**C6** and (−)-(*S*)-**C5**. As seen above, this latter must be corrected to (−)-(*R*)-**C5**. The wrong assignment seems to be due to a combination of a missing conformer for compound **C5** and a wrong result of matrix-method calculations on the single conformer considered. In fact, our TDDFT calculations on compound (*S*)-**C5** (Figure 2) gave an ECD spectrum very different from that shown in the original paper for the same configuration (see comparison in the Figure S5 in the Supporting Information). In particular, we predicted the first major ECD band at 220−240 nm to be positive for (*S*)-**C5** and not negative as previously found. This is true for both low-energy conformers (conf#1 and conf#2) of (*S*)-**C5**, as can be seen from their respective calculated ECD spectra shown in Figure 3. Our lowest-energy conformer conf#1 of **C5** corresponds to structure **3a** in the original paper; however, it has a positive calculated ECD band at 225 nm (Figure 3) opposite to that calculated at 240 nm for **3a** in the original paper.[12] This latter discrepancy seems to be the main reason for the observed failure. Additionally, our second most stable conformer (conf#2 of **C5**) contributes strongly to the first major ECD band despite its smaller population, because its calculated spectrum is much more intense than the lowest-energy conformer (conf#1) in the long-wavelength region (Figure 3). This second conformer was instead neglected in the previous investigation.[12]

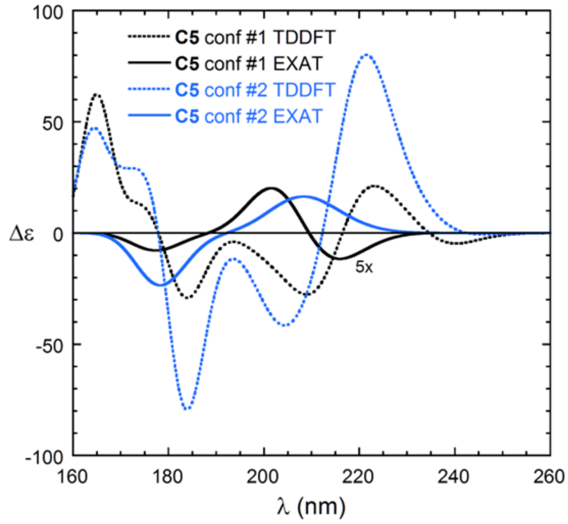

Figure 3. ECD spectra calculated for the two most stable conformers of (*S*)-**C5** with TDDFT (dotted lines) and EXAT matrix method (solid lines). In both cases, the level of theory was CAM-B3LYP/def2-TZVP. Spectra are convoluted as sums of Gaussians with 0.3 eV exponential half-width.

Trying to reproduce the original results, we ran ECD calculations with the tool EXAT (excitonic analysis tool) developed by Mennucci and co-workers.[37,40,41] EXAT represents a modern, more refined, and less approximated version of Schellman's matrix method. The main differences between our EXAT calculations and matrix-method calculations run by Sandström and co-workers are (1) diagonal terms were extracted from the aforementioned TDDFT calculations on model chromophores, rather than from experimental data, and (2) the off-diagonal terms (interchromophoric couplings) were evaluated using full TDDFT transition densities, instead of AM1-derived point charges. EXAT calculations were run using DFT-optimized geometries of (*S*)-**C5** and (*R*)-**C6** and the transition densities calculated with TDDFT at the CAM-B3LYP/def2-TZVP level for the model chromophores 1,2-dimethylbenzene and *N*-formylvinylamine (optimized at the *ω*B97X-D/6-311+G(d,p) level). In Figure 3, EXAT calculations for the two most stable conformers of (*S*)-**C5** are compared with full TDDFT calculations for the same structures. A similar comparison for (*R*)-**C6** is reported in Figure S6 in the Supporting Information.

Inspection of Figure 3 reveals that there is a large difference between the spectra calculated with the two methods for both conformers of (*S*)-**C5**. Not only the signs and relative intensities but also the positions and even the numbers of apparent bands are different. The fact that a TDDFT-based fragmentation approach led to very different results from full TDDFT calculations was a first hint that the two chromophores do not fulfill the requirements for the independent system approximation (ISA). A comparison between our EXAT and the original matrix-method results is shown in Figure S5 in the Supporting Information for the lowest energy conformer of (*S*)-**C5** (DFT structure **C5** conf#1 corresponding to structure **3a** in the original paper). Apart from the expected differences due to the different descriptions of transition densities, it is interesting to note that the pattern of signs obtained by the two methods is consistent. In particular, the first major ECD band is predicted to be positive for (*S*)-**C5** with both methods and is followed by a second negative band. Both bands appear to be reversed when full TDDFT calculations are employed (Figure S5 in the Supporting Information). Therefore, the matrix method, either in its traditional Schellman formulation or its modern EXAT version, is unable to calculate the ECD spectrum of **C5** correctly. The failure has then to be attributed to the nature of the system, which cannot be treated within the ISA framework, rather than to the specific description of transition densities or to the set of parameters used for point charges. In that respect, the correct absolute configuration assigned to (+)-(*R*)-**C6** in the original paper by means of the same calculations[12] must be regarded as fortuitous. In fact, for this compound a large difference was also observed between TDDFT- and EXAT-calculated ECD spectra (see Figure S6 in the Supporting Information).

Transitions and Orbital Analysis. To further demonstrate that the independent system approximation cannot be applied to the discussed compounds, we analyzed more in detail our TDDFT calculation results on (*S*)-**C5** and (*R*)-**C6**. The major calculated transitions for the lowest-energy conformer (conf#1) of (*S*)-**C5**, in terms of component single excitations, are reported in Table 1. The relevant frontier Kohn−Sham orbitals are shown in Figure 4. Most orbitals (in particular the bonding ones) are apparently localized on both chromophores, and in some cases a clear overlap between the benzene and amide orbitals is appreciable (see e.g. 54 and 55). Thus, the two chromophores cannot be considered "independent" at all: i.e., isolated from each other and nonconjugated. Moreover, the most diagnostic ECD band, that is the first and most intense ECD band observed around 240−250 nm, is not the result of an exciton coupling between the phenyl and *N*-vinyl amide chromophores, as assumed.[12,13] The two transitions occurring in this range with positive rotational strength (excited states 2 and 3 in Table 1) have in fact a large charge-transfer character (56 → 60 and 57 → 58 excitations). The same is true for the following transition with negative rotational strength (excited state 4, 57 → 58 and 57 → 59 excitations). A consistent situation was found for compound (*R*)-**C6**, for which the

Table 1. Analysis of the First Five Transitions Calculated for the Lowest-Energy Conformer of Compound (*S*)-C5 at the CAM-B3LYP/def2-TZVP//*ω*B97X-D/6-311+G(d,p) Level

exc state	λ/nm	$R/10^{-40}$ cgs[a]	exc[b]	exc coeff	Δr/Å[c]
1	235.46	−19.71	56 → 58	0.44633	1.79
			54 → 60	0.32841	
			55 → 59	0.28633	
2	231.51	+19.34	56 → 60	0.33022	2.00
			56 → 58	0.29190	
			54 → 60	−0.25631	
			55 → 59	0.23320	
3	220.72	+32.88	57 → 58	0.53606	2.85
			57 → 60	−0.42038	
4	212.04	−30.08	57 → 59	0.40967	2.83
			57 → 60	−0.36077	
			57 → 58	−0.33980	
5	206.90	−14.86	56 → 59	0.45853	1.72
			55 → 58	−0.39437	
			57 → 59	−0.20914	

[a] Rotational strengths calculated with the dipole-length formalism. [b] Only the single excitations with coefficients larger than 0.2 (absolute value) are given. The numbers refer to the Kohn−Sham orbitals shown in Figure 4. [c] Charge-transfer metric index defined in ref 43.

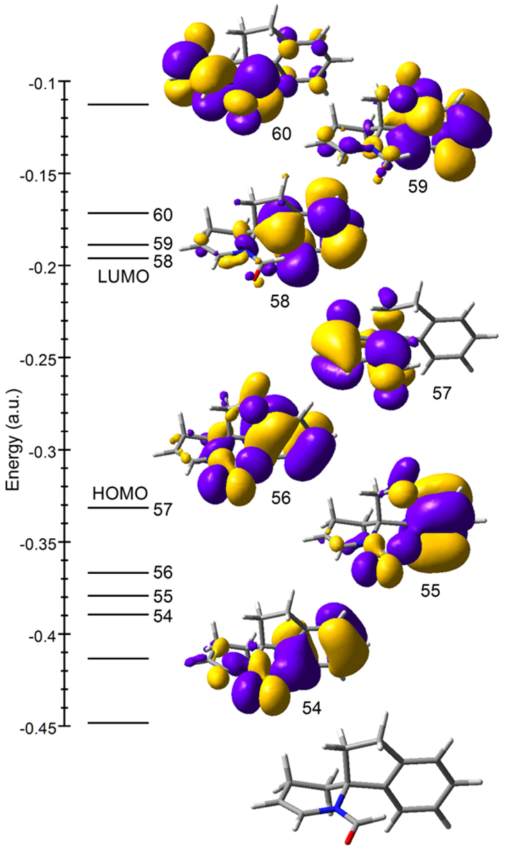

Figure 4. Frontier Kohn−Sham orbitals calculated for the lowest-energy conformer (conf#1) of compound (*S*)-**C5** (shown in the bottom) at the CAM-B3LYP/def2-TZVP//*ω*B97X-D/6-311+G(d,p) level. Orbitals are plotted with 0.02 isovalue.

transition analysis and relevant Kohn−Sham orbitals are reported in Table S2 in the Supporting Information. The charge-transfer (CT) character of the discussed transitions can be quantified by using a CT-metric measurement such as the Δr index introduced by Guido and co-workers.[42,43] This index corresponds to the average distance (expressed in Å) covered by the electron during the excitation. $\Delta r \geq 2$ Å indicates a substantial CT character and calls for caution in the use of TDDFT calculations, especially with some functionals.[33,42,43] As shown in Table 1, the three excited states 2−4 responsible for the two major ECD bands are allied with Δr between 2 and 2.8 Å, as estimated at the CAM-B3LYP/def2-TZVP level for the lowest-energy conformer (conf#1) of (*S*)-**C5**. Similar values were obtained for compound (*R*)-**C6** (Table S2 in the Supporting Information). Interestingly enough, Δr values evaluated at the B3LYP/def2-TZVP level are very high (between 3.5 and 4 Å) for the first two transitions of both (*S*)-**C5** and (*R*)-**C6** (Tables S3 and S4 in the Supporting Information). Thus, B3LYP overestimates the CT character of these transitions, which also explains the appearance of the calculated ECD spectra and their poorer agreement with the experiment (see Figure S1 in the Supporting Information). We confirm the known trend that range-separated functionals such as CAM-B3LYP, or global hybrids with a large HF exchange fraction such as M06-2X, are more suitable than B3LYP to calculate ECD spectra involving transitions with moderate CT character.[27,44,45]

It must be stressed that charge-transfer transitions require ad hoc parametrization to be included in matrix-method calculations,[46,47] which was employed neither in the original paper nor in the present EXAT calculations.

CONCLUSIONS

Molecules **C5** and **C6** do not represent “two compounds with similar configuration but nearly mirror image CD spectra”.[12] The ECD spectra are actually very similar for the same configuration: namely, (*S*)-**C5** and (*R*)-**C6** (recall the formal inversion of chirality according to the sequence rule). Of course, the final warning in the original paper about “the risk of deducing absolute configurations by a direct comparison of CD spectra”[12] is still entirely valid and has been demonstrated by other examples.[48,49] In contrast, it is not exemplified by the two analogous spiro compounds **C5** and **C6**, as originally stated and implied by several literature citations.[17−24]

Quantum-mechanical calculations with the TDDFT method revealed that the previous configurational assignment of compound **C5**, based on matrix-method calculations, was wrong. The revised absolute configuration is (−)-(*R*)-**C5**. A few inconsistencies in the previous investigation have emerged during our re-evaluation with more modern calculation methods. They include an important conformer missed by the MM2 conformational search, a slightly incorrect structure obtained by MM2 geometry optimization for the lowest-energy conformer, and incorrect transition charge monopoles found by AM1 calculations. None of these flaws seem crucial, however. The main reason for the incorrectness of the reported assignment is that the two spiro compounds **C5** and **C6** cannot be reasonably treated within the ISA framework, and their ECD spectra cannot be calculated by any kind of matrix method (which necessarily relies on the ISA).

This conclusion has implications which go beyond the specific case discussed here and are still valid in the present time. In fact, the observed failure is related to a wrong assumption on the validity of the ISA rather than to a limitation in the computational tools available 20 years ago. Fragmentation approaches are still very popular for the calculation of aggregate (chiro)optical properties through their modern implementations such as EXAT.[37,41,46,47,50−56] These calculation schemes take advantage of transition densities and other parameters calculated at ab initio or TDDFT levels. Their accuracy has therefore obviously much improved with respect to the traditional matrix methods, which relied on point−dipole or charge−monopole approximations. Still, any matrix method or fragmentation scheme is based on the same essential prerequisite, that is, the validity of the independent system approximation, which should never be taken for granted even in the case of apparently nonconjugated systems, and verified case by case.

COMPUTATIONAL SECTION

MM and preliminary DFT calculations were run with Spartan’14 (Wavefunction, Inc., Irvine, CA, 2014), with standard parameters and convergence criteria. DFT and TD-DFT calculations were run with Gaussian’09,[57] with default grids and convergence criteria. Conformational searches were run with the Monte Carlo algorithm implemented in Spartan’14 using the Merck molecular force field (MMFF).[58] All MMFF minima were optimized in vacuo at the DFT level, employing the ωB97X-D[59] functional and the 6-311+G(d,p) basis set. Only minima with Boltzmann population >1% at 300 K (estimated from internal energies) were considered for TDDFT calculations. For both compounds **C5** and **C6**, four minima fitting the above criterion were found (see Figure 1).

TDDFT calculations were run with the functionals B3LYP,[60] CAM-B3LYP,[61] and M06-2X[62] and with the def2-TZVP basis set,[63] either in vacuo or including the polarizable continuum solvent model in its integral equation formalism (IEF-PCM) for ethanol.[29] UV and ECD spectra were generated using the program SpecDis[64] by applying a Gaussian band shape with 0.3 eV exponential half-width, from dipole length rotational strengths. Optical rotations at the D line (589.3 nm) were estimated by dipole electric field polarizability calculations at the CAM-B3LYP/def2-TZVP level using IEF-PCM for ethanol.

Matrix-method calculations were run with the excitonic analysis tool (EXAT) developed by Mennucci and co-workers.[37,40,41] As input geometries, the two most stable conformers of compounds **C5** and **C6** were used, obtained by DFT geometry optimizations (see above). Transition parameters were extracted from TDDFT calculations on 1,2-dimethylbenzene and *N*-formylvinylamine. The geometries of the model compounds (single conformation) were optimized by DFT at the ωB97X-D/6-311+G(d,p) level. TDDFT calculations were then run at the CAM-B3LYP/def2-TZVP level in vacuo, and the sets of transition point charges were obtained by fitting the electrostatic potential generated by the TDDFT transition density, according to the Merz−Kollman scheme.[38,39] The Coulombic component of the electronic coupling has been calculated by integration of TDDFT transition densities as reported in ref 37. For 1,2-dimethylbenzene the first four transitions were considered ($\pi \rightarrow \pi^*$ transitions of ^1L_b, ^1L_a, ^1B_b, and ^1B_a type). For *N*-formylvinylamine the first two transitions were considered ($n \rightarrow \pi^*$ and $\pi \rightarrow \pi^*$ transitions). ECD spectra were generated as EXAT outputs by applying a Gaussian band shape with 0.3 eV exponential half-width. EXAT calculations were run by interfacing with a locally modified version of the Gaussian’09 package.

The Δr index calculations were run with the program Multiwfn, version 3.3.8.[65]

ASSOCIATED CONTENT

Supporting Information

The Supporting Information is available free of charge on the ACS Publications website at DOI: 10.1021/acs.joc.6b01416.

Original experimental and calculated spectra and parameters for the calculation of electronic couplings from ref 12, TDDFT-derived Merz−Kollman charges, additional data for compound **C6**, calculation results with B3LYP and M06-2X and including the PCM solvent model, and a comparison between our calculations and those reported in ref 12 (PDF)

AUTHOR INFORMATION

Corresponding Author

*E-mail for G.P.: gennaro.pescitelli@unipi.it

Notes

The authors declare no competing financial interest.

ACKNOWLEDGMENTS

We are grateful to Prof. B. Mennucci (University of Pisa) for access to development code.

REFERENCES

(1) Barron, L. D. *Molecular Light Scattering and Optical Acticity*; Cambridge University Press: Cambridge, U.K., 2004.

(2) *Circular Dichroism and the Conformational Analysis of Biomolecules*; Fasman, G. D., Ed.; Plenum Press: New York, 1996.

(3) Lightner, D. A.; Gurst, J. E. *Organic Conformational Analysis and Stereochemistry from Circular Dichroism*; Wiley: New York, 2000.

(4) Pescitelli, G.; Di Bari, L.; Berova, N. *Chem. Soc. Rev.* **2011**, *40*, 4603−4625.

(5) Di Bari, L.; Pescitelli, G.; Salvadori, P. *J. Am. Chem. Soc.* **1999**, *121*, 7998−8004.

(6) Ding, Y.; Li, X.-C.; Ferreira, D. *J. Org. Chem.* **2007**, *72*, 9010−9017.

(7) Mammana, A.; Pescitelli, G.; Asakawa, T.; Jockusch, S.; Petrovic, A. G.; Monaco, R. R.; Purrello, R.; Turro, N. J.; Nakanishi, K.; Ellestad, G. A.; Balaz, M.; Berova, N. *Chem. - Eur. J.* **2009**, *15*, 11853−11866.

(8) Polavarapu, P. L.; Jeirath, N.; Walia, S. *J. Phys. Chem. A* **2009**, *113*, 5423−5431.

(9) Shimizu, A.; Mori, T.; Inoue, Y.; Yamada, S. *J. Phys. Chem. A* **2009**, *113*, 8754−8764.

(10) Vorlíčková, M.; Kejnovská, I.; Sagi, J.; Renčiuk, D.; Bednářová, K.; Motlová, J.; Kypr, J. *Methods* **2012**, *57*, 64−75.

(11) Miyahara, T.; Nakatsuji, H. *J. Phys. Chem. A* **2013**, *117*, 14065−14074.

(12) Ripa, L.; Hallberg, A.; Sandström, J. *J. Am. Chem. Soc.* **1997**, *119*, 5701−5705.

(13) Sandström, J. *Chirality* **2000**, *12*, 162−171.

(14) Sandström, J. In *Circular Dichroism-Principles and Applications*, 2nd ed.; Berova, N. N., Koji, Woody, R. W., Eds.; Wiley-VCH: New York, 2000; p 459−490.

(15) Madison, V.; Schellman, J. *Biopolymers* **1972**, *11*, 1041−1076.

(16) Raabe, G.; Fleischhauer, J.; Woody, R. W. In *Comprehensive Chiroptical Spectroscopy*; Berova, N., Polavarapu, P. L., Nakanishi, K., Woody, R. W., Eds.; Wiley: New York, 2012; Vol. *1*, pp 543−591.

(17) Ziegler, M.; von Zelewsky, A. *Coord. Chem. Rev.* **1998**, *177*, 257−300.

(18) Donnoli, M. I.; Scafato, P.; Superchi, S.; Rosini, C. *Chirality* **2001**, *13*, 258−265.

(19) Devlin, F. J.; Stephens, P. J.; Scafato, P.; Superchi, S.; Rosini, C. *Chirality* **2002**, *14*, 400−406.

(20) Dondoni, A.; Massi, A.; Minghini, E.; Bertolasi, V. *Helv. Chim. Acta* **2002**, *85*, 3331−3348.

(21) Dondoni, A.; Massi, A.; Sabbatini, S.; Bertolasi, V. *J. Org. Chem.* **2002**, *67*, 6979−6994.

(22) Dondoni, A.; Massi, A.; Minghini, E.; Sabbatini, S.; Bertolasi, V. *J. Org. Chem.* **2003**, *68*, 6172−6183.

(23) Berova, N.; Di Bari, L.; Pescitelli, G. *Chem. Soc. Rev.* **2007**, *36*, 914−931.

(24) Coughlin, F. J.; Oyler, K. D.; Pascal, R. A.; Bernhard, S. *Inorg. Chem.* **2008**, *47*, 974−979.

(25) Uray, G.; Verdino, P.; Belaj, F.; Kappe, C. O.; Fabian, W. M. F. *J. Org. Chem.* **2001**, *66*, 6685−6694.

(26) Pescitelli, G. In *XXXV "A. Corbella" Summer School*; Società Chimica Italiana: Gargnano (BS), Italy, 2002; pp 105−128.

(27) Pescitelli, G.; Bruhn, T. *Chirality* **2016**, *28*, 466−474.

(28) Mennucci, B.; Cappelli, C.; Cammi, R.; Tomasi, J. *Chirality* **2011**, *23*, 717−729.

(29) *Continuum Solvation Models in Chemical Physics: From Theory to Applications*; Mennucci, B., Cammi, R., Eds.; Wiley: Chichester, U.K., 2007.

(30) Polavarapu, P. L. *Chirality* **2016**, *28*, 445−452.

(31) Dreuw, A.; Head-Gordon, M. *J. Am. Chem. Soc.* **2004**, *126*, 4007−4016.

(32) Dreuw, A.; Head-Gordon, M. *Chem. Rev.* **2005**, *105*, 4009−4037.

(33) Le Bahers, T.; Adamo, C.; Ciofini, I. *J. Chem. Theory Comput.* **2011**, *7*, 2498−2506.

(34) Adamo, C.; Jacquemin, D. *Chem. Soc. Rev.* **2013**, *42*, 845−856.

(35) Pescitelli, G.; Gabriel, S.; Wang, Y.; Fleischhauer, J.; Woody, R. W.; Berova, N. *J. Am. Chem. Soc.* **2003**, *125*, 7613−7628.

(36) Kenny, E. P.; Kassal, I. *J. Phys. Chem. B* **2016**, *120*, 25−32.

(37) Jurinovich, S.; Pescitelli, G.; Di Bari, L.; Mennucci, B. *Phys. Chem. Chem. Phys.* **2014**, *16*, 16407−16418.

(38) Besler, B. H.; Merz, K. M.; Kollman, P. A. *J. Comput. Chem.* **1990**, *11*, 431−439.

(39) Singh, U. C.; Kollman, P. A. *J. Comput. Chem.* **1984**, *5*, 129−145.

(40) Jurinovich, S.; Guido, C. A.; Mennucci, B. *EXAT (Excitonic Analysis Tool)*; University of Pisa, Pisa, Italy, 2014; https://www1.dcci.unipi.it/molecolab/tools/.

(41) Jurinovich, S.; Guido, C. A.; Bruhn, T.; Pescitelli, G.; Mennucci, B. *Chem. Commun.* **2015**, *51*, 10498−10501.

(42) Guido, C. A.; Cortona, P.; Adamo, C. *J. Chem. Phys.* **2014**, *140*, 104101.

(43) Guido, C. A.; Cortona, P.; Mennucci, B.; Adamo, C. *J. Chem. Theory Comput.* **2013**, *9*, 3118−3126.

(44) Berardozzi, R.; Guido, C. A.; Capozzi, M. A. M.; Cardellicchio, C.; Di Bari, L.; Pescitelli, G. *Eur. J. Org. Chem.* **2015**, *2015*, 5554−5562.

(45) Bruhn, T.; Witterauf, F.; Götz, D. C. G.; Grimmer, C. T.; Würtemberger, M.; Radius, U.; Bringmann, G. *Chem. - Eur. J.* **2014**, *20*, 3998−4006.

(46) Oakley, M. T.; Hirst, J. D. *J. Am. Chem. Soc.* **2006**, *128*, 12414−12415.

(47) Bulheller, B. M.; Miles, A. J.; Wallace, B. A.; Hirst, J. D. *J. Phys. Chem. B* **2008**, *112*, 1866−1874.

(48) Kosaka, M.; Kuwahara, S.; Watanabe, M.; Harada, N.; Job, G. E.; Pirkle, W. H. *Enantiomer* **2002**, *7*, 213−7.

(49) Harada, N.; Kuwahara, S. In *Comprehensive Chiroptical Spectroscopy*; Berova, N., Polavarapu, P. L., Nakanishi, K., Woody, R. W., Eds.; Wiley: New York, 2012; Vol. *2*, pp 167−215.

(50) Bruhn, T.; Pescitelli, G.; Jurinovich, S.; Schaumlöffel, A.; Witterauf, F.; Ahrens, J.; Bröring, M.; Bringmann, G. *Angew. Chem., Int. Ed.* **2014**, *53*, 14592−14595.

(51) Loco, D.; Jurinovich, S.; Bari, L. D.; Mennucci, B. *Phys. Chem. Chem. Phys.* **2016**, *18*, 866−877.

(52) Jurinovich, S.; Curutchet, C.; Mennucci, B. *ChemPhysChem* **2014**, *15*, 3194−3204.

(53) Di Meo, F.; Pedersen, M. N.; Rubio-Magnieto, J.; Surin, M.; Linares, M.; Norman, P. *J. Phys. Chem. Lett.* **2015**, *6*, 355−359.

(54) Neugebauer, J.; Veldstra, J.; Buda, F. *J. Phys. Chem. B* **2011**, *115*, 3216−3225.

(55) Bulheller, B. M.; Rodger, A.; Hirst, J. D. *Phys. Chem. Chem. Phys.* **2007**, *9*, 2020−2035.

(56) Jiang, J.; Abramavicius, D.; Bulheller, B. M.; Hirst, J. D.; Mukamel, S. *J. Phys. Chem. B* **2010**, *114*, 8270−8277.

(57) Frisch, M. J.; Trucks, G. W.; Schlegel, H. B.; Scuseria, G. E.; Robb, M. A.; Cheeseman, J. R.; Scalmani, G.; Barone, V.; Mennucci, B.; Petersson, G. A.; Nakatsuji, H.; Caricato, M.; Li, X.; Hratchian, H.

DOI: 10.1021/acs.joc.6b01416
J. Org. Chem. 2016, 81, 7725−7732

P.; Izmaylov, A. F.; Bloino, J.; Zheng, G.; Sonnemberg, J. L.; Hada, M.; Ehara, M.; Toyota, K.; Fukuda, R.; Hasegawa, J.; Ishida, M.; Nakajima, T.; Honda, Y.; Kitao, O.; Nakai, H.; Vreven, T.; Montgomery, J. A., Jr.; Peralta, J. E.; Ogliaro, F.; Bearpark, M.; Heyd, J. J.; Brothers, E.; Kudin, K. N.; Staroverov, V. N.; Kobayashi, R.; Normand, J.; Raghavachari, K.; Rendell, A.; Burant, J. C.; Iyengar, S. S.; Tomasi, J.; Cossi, M.; Rega, N.; Millam, J. M.; Klene, M.; Knox, J. E.; Cross, J. B.; Bakken, V.; Adamo, C.; Jaramillo, J.; Gomperts, R.; Stratmann, R. E.; Yazyev, O.; Austin, A. J.; Cammi, R.; Pomelli, C.; Ochterski, J. W.; Martin, R. L.; Morokuma, K.; Zakrzewski, V. G.; Voth, G. A.; Salvador, P.; Dannenberg, J. J.; Dapprich, S.; Daniels, A. D.; Farkas, O.; Foresman, J. B.; Ortiz, J. V.; Cioslowski, J.; Fox, D. J. *Gaussian 09, Revision D.01*; Gaussian, Inc., Wallingford, CT, 2013.

(58) Halgren, T. A. *J. Comput. Chem.* **1996**, *17*, 490−519.

(59) Chai, J.-D.; Head-Gordon, M. *Phys. Chem. Chem. Phys.* **2008**, *10*, 6615−6620.

(60) Becke, A. D. *J. Chem. Phys.* **1993**, *98*, 5648−5652.

(61) Yanai, T.; Tew, D. P.; Handy, N. C. *Chem. Phys. Lett.* **2004**, *393*, 51−57.

(62) Zhao, Y.; Truhlar, D. G. *Theor. Chem. Acc.* **2008**, *120*, 215−241.

(63) Weigend, F.; Ahlrichs, R. *Phys. Chem. Chem. Phys.* **2005**, *7*, 3297−3305.

(64) Bruhn, T.; Schaumlöffel, A.; Hemberger, Y.; Bringmann, G. *Chirality* **2013**, *25*, 243−249.

(65) Lu, T.; Chen, F. *J. Comput. Chem.* **2012**, *33*, 580−592.